ASIAN JOURNAL OF CIVIL ENGINEERING (BHRC) VOL. 18, NO. 4(2017)
PAGES 567-575

INVESTIGATION OF MODE II IN FOUR POINT BENDING BEAM TEST

S.J. Jung[1*] and Ahmad M. Abu Abdo[2]
[1]Department of Civil Engineering, University of Idaho, P.O. Box 441022, Moscow, ID 83844-1022, USA
[2]Department of Civil & Infrastructure Engineering, American University of Ras Al Khaimah, PO Box 10021, Ras Al Khaimah, UAE

Received: 25 September 2016; **Accepted:** 27 November 2016

ABSTRACT

A Finite Element Analysis has been applied to a type of four-point bending specimen with S/W=3 to determine which condition a pure mode II can be constructed. The ANSYS simulation results have demonstrated that conditions $l_1 = l_4$ and $l_2 = l_3$ could not guarantee a pure mode II case be generated. The ratio W/D and ratio a/W have a remarkable contribution to the formation of pure mode II. At W/D = 3.75 and a/W from 0.25 to 0.35, an almost perfect shear mode II can be achieved at the single crack tip region. When a/W varies 0.2 to 0.6, the specimen can also be treated as in pure shear mode II case if a 6 percent of the ratio K_I/K_{II} is acceptable. A K_{II} expression in fifth-degree polynomials has been calibrated.

Keywords: Fracture mechanics; four-point bending; stress intensity factor; mode II fracture; finite element analysis.

1. INTRODUCTION

One of the most commonly used specimens in the study of mode II is the four-point bending specimen. This specimen testing setup has investigated in many studies [1-8]. Different researchers may take different specimen configuration, but all the specimens meet the conditions which are that $l_1 = l_4$ and $l_2 = l_3$, shown in Fig. 1. The reason to do so is that meeting this condition will lead a zero bending moment M but a non-zero shear force Q along the crack surface direction. And on these specific conditions, some researchers believe that a pure shear mode II will be produced in the crack tip region [9]. Some researchers, however, have variously mentioned that the stress intensity factor mode II is much greater than mode I ($K_{II} >> K_I$) but have not given reason to be so. Also, none of these researchers have provided the magnitude of K_I, K_{II} and the ratio of K_I/K_{II} to give us a clear vision how is $K_{II} >> K_I$.

*E-mail address of the corresponding author: sjung@uidaho.edu (S.J. Jung)

The purpose of this investigation has been to develop a finite element analysis to study the four-point bending specimen to verify whether or not a pure mode II will always be generated in the crack tip when the above conditions $l_1 = l_4$ and $l_2 = l_3$ are met. If not, is it possible to induce a pure mode II in this four-point bending specimen and what are the conditions to produce a pure mode II. This research is also going to calibrate K_{II} expression form with crack length since so far none of such studies have been done.

2. FINITE ELEMENT ANALYSIS

Many studies have been conducted different test setups using numerical techniques (e.g. Finite Element Method) [10-18] Blandford et al. [18] had investigated four-point bending specimen by using boundary element method. However, he only analyzed Mode I case produced by the bending moment M and compared his results with those of Brown and Srawley [19] by boundary collocation K calibrations. In this paper, a finite element method; ANSYS has been used to investigate mainly the Mode II case.

The specimen size and loading configuration are shown in Fig. 1. The specimen length is 44 cm. During ANSYS simulation, we take the specimen with $l_1 = l_4 = D$ and $l_3 = l_2 = L$ so above conditions are met. And also let S = 36 cm; specimen width W = 12 cm; S/W = 3; L = 18 cm; and $d_1 = d_2 = 4$ cm. Crack length a and distance D were variable in different simulation. A typical finite element model is shown in Fig. 2 which consists of 3935 PLANE82 elements and 11604 nodes for the specimen that D = 2.0 cm and a = 3.5 cm.

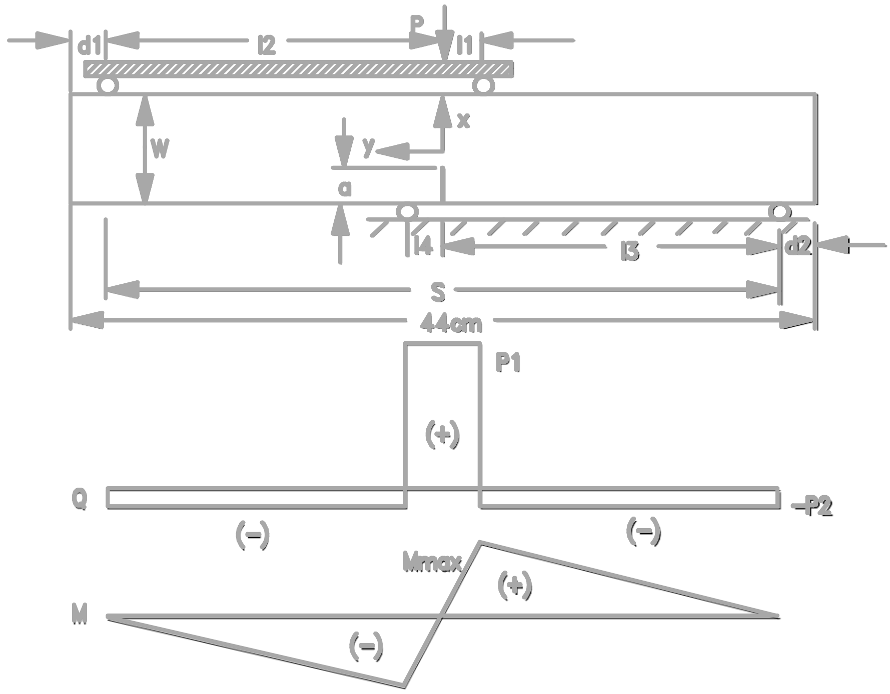

Figure 1. Four-point Bending Specimen and Simplified Stress State

Generally, the specimen can be treated as in a mixed case of mode I and mode II. Therefore the crack tip stresses could be expressed as the following equations:

$$\sigma_x = \frac{K_I}{\sqrt{2\pi r}} \cos\frac{\theta}{2}\left(1 - \sin\frac{\theta}{2}\sin\frac{3\theta}{2}\right) - \sigma - \frac{K_{II}}{\sqrt{2\pi r}} \sin\frac{\theta}{2}\left[2 + \cos\frac{\theta}{2}\cos\frac{3\theta}{2}\right] \tag{1}$$

$$\sigma_y = \frac{K_I}{\sqrt{2\pi r}} \cos\frac{\theta}{2}\left(1 + \sin\frac{\theta}{2}\sin\frac{3\theta}{2}\right) + \frac{K_{II}}{\sqrt{2\pi r}} \sin\frac{\theta}{2}\cos\frac{\theta}{2}\cos\frac{3\theta}{2} \tag{2}$$

$$\tau_{xy} = \frac{K_I}{\sqrt{2\pi r}} \sin\frac{\theta}{2}\cos\frac{\theta}{2}\cos\frac{3\theta}{2} + \frac{K_{II}}{\sqrt{2\pi r}} \cos\frac{\theta}{2}\left[1 - \sin\frac{\theta}{2}\sin\frac{3\theta}{2}\right] \tag{3}$$

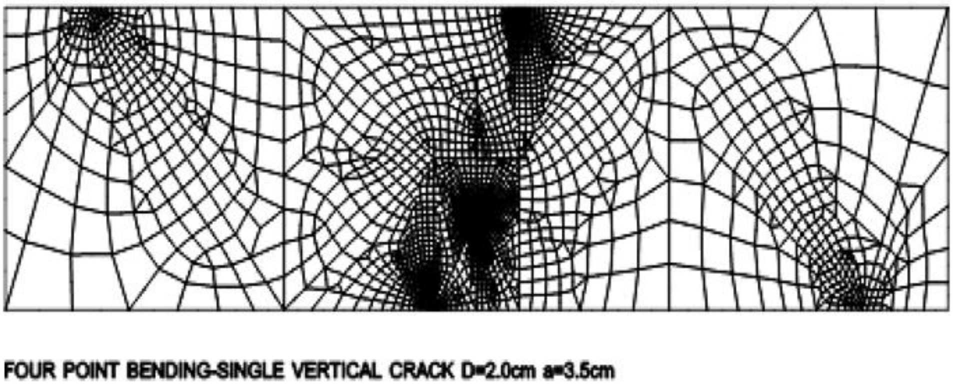

Figure 2. Mesh layout of the four-point bending model

The stress intensity factor K_I is obtained, as discussed by Chan et al. [20], from the stress method by an extrapolation of K_I^* from Eq. 2 and K_{II} is obtained by an extrapolation of K_{II}^* from Eq. 3.

3. RESULTS AND DISCUSSIONS

3.1 The effect of D

A set of simulations has been performed for six different D which varies from 2.0 cm to 4.8 cm while crack length a keeps being a constant 3.5 cm. The results are shown in Fig. 3 in terms of K_I/P, K_{II}/P and the ratio of K_I/K_{II}. P is the overall load.

From Fig. 3, it has been observed that at D=4.8 cm, K_I/P = 27.48 $m^{-3/2}$, K_{II}/P = 151.10 $m^{3/2}$ and the ration K_I/K_{II} is about 18.19 percent, then, as D decreases K_I/P will also decrease while K_{II}/P will increase. At D = 3.2 cm, K_I/P = -0.80 $m^{-3/2}$, K_{II}/P = 197.31 $m^{-3/2}$ and the ration K_I/K_{II} we get is as small as -0.41 percent. In this specimen loading configuration, we believe that a pure mode II specimen has been produced. As D continuously decrease, K_{II}/P

keeps increasing while K_I/P keeps decreasing and takes negative values. But the absolute value of K_I/P is increasing, so is the ratio of K_I/K_{II}. Therefore, the specimen is also away from the pure mode II. It is not surprising that K_I can be negative. In fact, Swartz [7] had also got negative K_I in the four-point bending specimen.

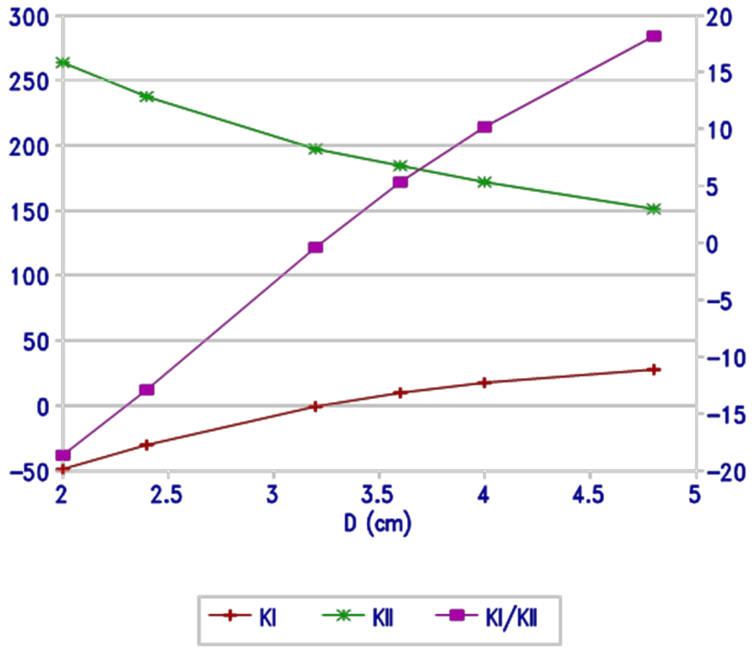

Figure 1. K_I/P, K_{II}/P, and K_I/K_{II} variation with D

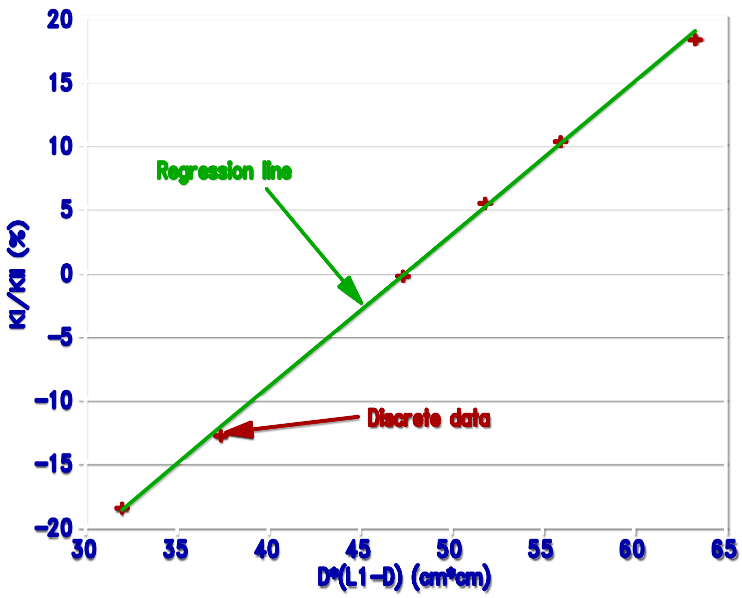

Figure 2. Linear relationship between K_I/K_{II} and D

Therefore, ANSYS simulation results demonstrate that on the conditions $l_1 = l_4$, $l_2 = l_3$, K_I (K_I/P) is not always zero. In fact, only at one point D equal about 3.2 cm, the K_I value is zero which is strictly pure shear mode II for a/W =0.292. Other than that, both modes I and mode II exist theoretically.

Further analysis demonstrates that it seems a linear relationship between the ratio K_I/K_{II} and the $D(L_1\text{-}D)$, here $L_1 = L - D$, shown in Fig. 4. A regression line is obtained as below:

$$\frac{K_I}{K_{II}}=1.20x10^4 D(L_1\text{-}D)\text{-}57.14 \tag{4}$$

Where, the unit of D and L_1 are in meters.

For experimental convenience, if the crack tip with 6 percent of K_I/K_{II} is acceptable to be treated as pure mode II, the D range is from 3.0 cm to 3.6 cm. Or maybe more importantly, W/D range is from 4 down to 10/3.

3.2 Crack length (a)

Since at D = 3.2 cm (W/D = 3.75), the smallest ratio K_I/K_{II} is provoked. We have more interesting on this loading configuration. At D = 3.2 cm, let crack length vary from 0.6 cm to 7.2 cm (a/W ranges from 0.2 to 0.6), another set of ANSYS simulations with 12 different a has been done. Table 1 shows the simulation results.

Table 1: K_I/P, K_{II}/P, and K_I/K_{II} with different a/W (P in pounds, K_I & K_{II} in lb.m$^{-3/2}$)

a (m)	a/W	K_I/P from ANSYS	K_{II}/P from ANSYS	K_I/K_{II} (%)	K_{II}/P From Eq. 5	Error (%)
0.006	0.05	52.03	12.14	428.58	-	
0.012	0.10	38.60	41.48	93.06	-	
0.018	0.15	20.35	81.46	24.98	-	
0.024	0.20	7.19	132.00	5.45	132.08	0.06
0.030	0.25	0.58	166.82	0.35	166.70	-0.07
0.035	0.292	-0.80	197.31	-0.41	197.31	0
0.042	0.35	1.09	239.39	0.46	239.14	-0.10
0.048	0.40	4.95	273.43	1.81	272.65	-0.29
0.054	0.45	9.79	304.31	3.22	304.61	0.10
0.060	0.50	14.80	338.38	4.37	337.51	-0.26
0.066	0.55	19.95	374.15	5.33	374.37	0.06
0.072	0.60	24.35	415.34	5.86	415.97	0.15

It has been observed that at a/W = 0.1, K_I/P equals to 38.60 m$^{-3/2}$ while K_{II}/P equals to 41.48 m$^{-3/2}$, both of them are about as same. At a/W = 0.05, K_I/P equals to 52.03 m$^{-3/2}$ which is much bigger than K_{II}/P with 12.14 m$^{-3/2}$. Obviously, the specimen crack tip absolutely cannot be treated as pure mode II in these cases. However, if a 6 percent of K_I/K_{II} is acceptable, the specimen with a/W bigger than 0.2 can be treated as in mode II case, see in

Fig. 5. When a/W varies from 0.25 to 0.35, an almost perfect pure mode II case can be accomplished and the ratio K_I/K_{II} is less than 0.5 percent according to ANSYS results. These specimen geometries a/W from 0.25 to 0.35 are highly recommended for the four-point bending specimen.

Furthermore, while a/W varies from 0.2 to 0.6, K_{II} can be represented by the following fifth-degree polynomials form:

$$K_{II}=Y\frac{L_1}{S\text{-}L_1}\frac{P\sqrt{\pi a}}{(W\text{-}a)B} \tag{5}$$

while

$$Y=1.12\text{-}9.25\frac{a}{W}+61.37\left(\frac{a}{W}\right)^2\text{-}172.35\left(\frac{a}{W}\right)^3+217.94\left(\frac{a}{W}\right)^4\text{-}103.90\left(\frac{a}{W}\right)^5 \tag{6}$$

where B is the specimen width; all length unit is in meters; P in pounds, and K_{II} in lb.m$^{-3/2}$.

The calculated K_{II} data based on Eq. 5 are also listed in Table 1 to compare with those from ANSYS. Those two sets of data are in excellent agreement with each other. Y (Eq. 6) curve is shown in Fig. 6. Unlike three-point bending specimen for Mode I in which Y curve is up parabola according to Brown and Srawley [19], Y curve in four-point bending specimen for Mode II is down parabola.

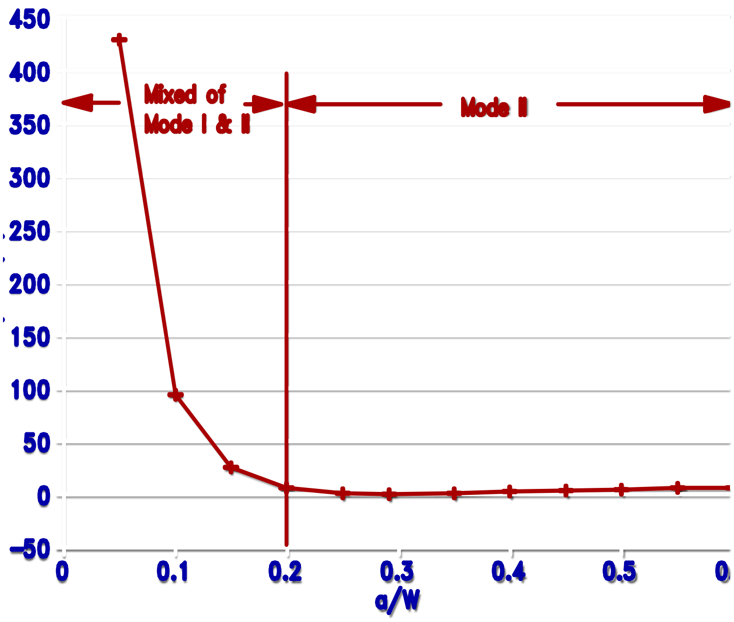

Figure 5. The ratio K_I/K_{II} with different a/W

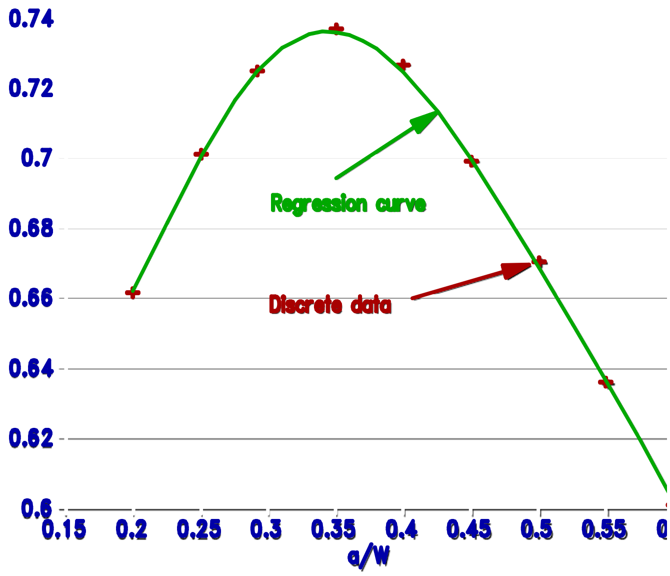

Figure 3. K_{II} Calibrations for four-point bending specimen (S/W=3)

4. CONCLUSIONS

Based on the results presented in this study, the following conclusions are made:

Meeting the conditions $l_1 = l_4$ and $l_2 = l_3$ does not guarantee a pure shear Mode II case will be achieved. The values of ratio W/D and ratio a/W have a remarkable contribution to the formation of pure Mode II.

For a type of four-point bending specimen with S/W = 3, at W/D = 3.75 and a/W from 0.25 to 0.35, an almost perfect Mode II can be achieved at the single crack tip region. This specimen geometry is highly recommended.

When a/W varies 0.2 to 0.6, the specimen can also be treated as in pure Mode II case and the ratio K_I/K_{II} is less than 6 percent. And K_{II} can be expressed in the following form:

$$K_{II}=Y\frac{L_1}{S-L_1}\frac{P\sqrt{\pi a}}{(W-a)B} \tag{7}$$

and

$$Y=1.12-9.25\frac{a}{W}+61.37\left(\frac{a}{W}\right)^2-172.35\left(\frac{a}{W}\right)^3+217.94\left(\frac{a}{W}\right)^4-103.90\left(\frac{a}{W}\right)^5 \tag{8}$$

REFERENCES

1. Ingraffea AR. Mixed mode fracture initiation in Indiana limestone and Westerly granite,

Proceedings of the 22nd U.S. Symposium on Rock Mechanics, Cambridge, MA, 1981, pp. 186-191.

2. Ingraffea AR, Asce M, Panthaki MJ, Asce AM. Analysis of "shear fracture" tests of concrete beams, finite element analysis of reinforced concrete structures, *Proceedings of the Seminar Sponsored by the Japan Society for the Promotion of Science and the U.S. National Science Foundation*, Tokyo, Japan, 1985, pp. 174-183.
3. Huang J, Wang S. An Experimental investigation concerning the comprehensive fracture toughness of some brittle rocks, *International Journal of Rock Mechanics and Mining Sciences & Geomechanics Abstracts*, No. 2, **22**(1985) 99-104.
4. Bazant ZP, Pfeiffer PA. Tests of the shear fracture and strain-softening in concrete, *Proceedings of the 2nd Symposium on the International on Non-Nuclear Munitions with Structures*, Panama City Beach, Florida, April 1985, pp. 15-19.
5. Bazant ZP, Pfeiffer PA. Shear fracture tests of concrete, *Materiaux ET Constructions*, No. 110, **19**(1986) 111-21.
6. Swartz SE, Lu LW, Tang LD, Refai TME. Mode II fracture-parameter estimates for concrete from beam specimens, *Experimental Mechanics*, No. 2, **28**(1988) 146-53.
7. Swartz SE, Taha NM. Mixed mode crack propagation and fracture in concrete, *Engineering Fracture Mechanics*, Nos. 1-3, **35**(1990) 137-44.
8. Jung SJ, Ba H, Whyatt, JK. Analysis of the KII mode shear fracture toughness for brittle materials", *The 43rd US Rock Mechanics Symposium and 4th U.S.-Canada Rock Mechanics Symposium*, Asheville, NC, USA June 28th–July 1, 2009.
9. Whittaker BN, Singh RN, Sun G, *Rock Fracture Mechanics, Principles, Design and Applications*, Elsevier, Amsterdam, 1992.
10. Li X. Finite element analysis of slope stability using a nonlinear failure criterion, *Computers and Geotechnics*, No. 3, **34**(2007) 127-36.
11. Zhao Z, Wang X. Evaluation of potential failure of rock slope at the left abutment of Jinsha river bridge by model test and numerical method, *Frontiers of Structural and Civil Engineering*, No. 3, **7**(2013) 332-40.
12. Steada D, Eberhardtb E, Cogganc JS. Developments in the characterization of complex rock slope deformation and failure using numerical modeling techniques, *Engineering Geology*, Nos. 1-3, **83**(2006) 217-35.
13. Li Y, Qiao L, Sui ZL, Li QW. Strength analysis of rock material under the brittle shear failure mode, *Jour. of Central South University of Technology*, No. 4, **16**(2009) 663-8.
14. Li Y, Li Z, Xu TJ. Research of brittle shear failure strength of rock materials, *Applied Mechanics and Materials*, **454**(2014) 125-8.
15. Eckwright F, Jung SJ, Abu Abdo AM. Utilizing a particle flow code in 2 dimensional discrete element method of fracture resistance evaluation of HMA and brittle rock, *Asian Journal of Civil Engineering (BHRC)*, No. 1, **15**(2014) 9-21.
16. Wang D, Zhang Z, Ge X. Study on shear failure behavior of embedded cracks subjected to different normal stresses, *Proceedings of Geo-Shanghai: Rock Mechanics and Its Applications in Civil, Mining, and Petroleum Engineering*, 2014, pp. 79-88.
17. Li Y, Zhou H, Zhu W, Li S, Liu J. Experimental and numerical investigations on the shear behavior of a jointed rock mass", *Geosciences Journal*, in press (2015) 1-9. DOI 10.1007/s12303-015-0052-z.

18. Blandford GE, Ingraffea AR. Two-dimensional stress intensity factor computations using the boundary element method, *International Journal for Numerical Methods in Engineering*, **17**(1981) 387-404.
19. Brown WF, Srawley JE. *Plane Strain Crack Toughness Testing of High Strength Metallic Materials*, ASTM Special Technical Publication STP 410, USA, 1966.
20. Chan SK, Tuba IS, Wilson WK. On the finite element method in linear fracture mechanics, *Engineering Fracture Mechanics*, **2**(1970) 1-17.